Article:
Royston, S.J., Strickland, D., Stone, D.A. orcid.org/0000-0002-5770-3917 et al. (3 more authors) (2020) Practical observations of loss-of-mains nuisance tripping of fast acting energy storage. International Journal of Smart Grid and Clean Energy, 9 (3). pp. 473-484. ISSN 2315-4462

10.12720/sgce.9.3.473-484

International Journal of Smart Grid and Clean Energy

Practical observations of loss-of-mains nuisance tripping of fast acting energy storage

Simon J Royston[a], Dani Strickland[b], David A Stone[a], Daniel T Gladwin[a], Martin P Foster[a], Shahab Nejad[a]

[a] *Department of Engineering, University of Sheffield, 3 Solly Street, Sheffield S1 4EP, UK*
[b] *Department of Engineering, Loughborough University, Wolfson Building Ashby Road, Loughborough LE11 3TU, UK*

Abstract

Fast acting battery energy storage systems are able to swing power very quickly between maximum import and maximum export in less than 50ms based on operational experience of a 2MW energy storage system. However, this can result in nuisance tripping of the unit through the operation of the loss-of-mains protection (LoM). This paper looks at data captured during power swings of up to 4MW during typical operation and discusses the potential for nuisance tripping, and suggests potential settings for improved operation.

Keywords: Power system protection, energy storage, energy management

1. Introduction

Fast acting energy storage systems (ESS) are connected to the grid in compliance with the same regulations used for connecting embedded generation, potentially causing nuisance tripping on ESS. In the UK, new draft standards for exporting energy to the National Grid are the Energy Networks Association (ENA) Engineering Recommendation G98 for units with a capacity less than 50kW(3-phase) or 17kW(1-phase) and the ENA Engineering Recommendation G99 for larger units. These are currently in draft form and are superseding the G83 [1]and G59 [2], respectively. These standards include technical requirements such as protection settings, compliance and commissioning necessities, which must be adhered to in order to export energy to the grid. The protection mechanisms of the G99 standard include 2-stage under-voltage, over-voltage, under-frequency and over-frequency, as well as an approved loss-of-mains (LoM)/anti-islanding protection method. LoM is designed to prevent a generator from unintentionally operating in an islanded mode when the grid system trips out and inadvertently energises parts of the Network. A setting map determined through modelling for synchronous generators has been proposed to maximise islanding detection, whilst reducing incorrect tripping to other events using traditional relay devices; this aim is more complex than can be dealt with through a standard [3]. Energy storage systems have the ability to provide power within a few cycles, much faster than possible with synchronous generators. ESS operate with different characteristics to synchronous generators meaning existing LoM could cause nuisance tripping of ESS.

The only methods of LoM protection currently allowed within the UK standards are rate of change of frequency (RoCoF) and vector shift. Research has been carried out into the continuing viability of these methods for loss-of-mains protection [4] and analytical tools have been developed from a real-world case study for determining LoM settings [5].

The National Grid Working Group GC0035/GC0079 [6] is currently undertaking a review of the settings. The proposed changes include increases to the RoCoF protection settings and the removal of the

* Manuscript received January 17th, 2019; revised February 10th 2020.
Corresponding author. *E-mail address*: s.royston@sheffield.ac.uk
doi: 10.12720/sgce.9.3.473-484

vector shift technique. The settings include an increase from the existing 0.125Hz/s to 1Hz/s with the requirement to operate over a period of 500ms. This is in response to the LoM sensitivity to network disturbances causing spurious disconnections and to improve fault ride through of connected generation units [7].

A number of alternative methods to RoCoF and vector shift have been proposed in literature that could be implemented to provide benefits for the operation of ESS. However, these tend to be more complex to implement. A review of the available methods is included in [8]. Examples of passive techniques include: Differentiating between phase steps and islanding conditions [4], comparing the RoCoF at multiple points on the system to differentiate between a local disturbance and a mains failure; known as change of rate of change of frequency (CoRoCoF) [9], continuous monitoring of the rate of change of voltage and change in power factor [10] and estimating oscillation frequency (though it is only useful for synchronous generators) [11].

Active techniques generally involve the generator adding a perturbation signal to its output. The system then decides if an islanding condition is present by the system response to the signal. These active methods can provide a more reliable indication of an islanding condition and result in a smaller non-detection zone. There can be drawbacks such as lowering the power quality on the bus they are connected to and can affect other systems utilising anti-islanding detection. A method of implementing RoCoF as an active technique has been proposed utilising low-frequency current injection [12]. Further active methods include frequency bias [13], active frequency drift [14], frequency jump [15], reactive error export detection [16], [17] and system impedance monitoring [18]. Another potential method uses fault level monitoring [19], which utilises thyristor switching to measure the current through a shunt inductor and thus calculate the fault level. None of these techniques are currently available for use in the UK, therefore they will not be considered in this study.

It is important that LoM protection is accurate, as unintentional islanding can be prolonged due to external factors. For example, under-frequency load shedding can prolong islanding conditions found from investigating naturally occurring substation, transmission and feeder events on the distribution network [20]. The events investigated look at traditional synchronous generation and wind farms, which have different characteristics to energy storage. Solar generation was considered – which has closer characteristics to energy storage – however insufficient data was available for a detailed study. Anti-islanding protection has also been shown to cause voltage sag in the local network [21]. Voltage sags can adversely affect the network and potentially cause additional maloperations in other distributed generation (DG) units.

The accuracy of LoM can be affected by external factors including white noise, which has been shown to introduce errors into the measurement of differentiated measurement methods such as RoCoF depending on the filtering method utilised [22]. Imbalance between the phases of the three-phase network can affect the LoM measurements. RoCoF is particularly sensitive to phase-angle unbalance [23]. The reliability of the anti-islanding protection can be optimised by managing the settings and network data using simulations. However, this is time consuming to carry out for individual cases and is only applicable to synchronous generation units [24].

A number of different methods have been proposed to improve the accuracy of RoCoF, including improving the filter method for RoCoF [23] along with a method of inserting capacitors onto the network when the main breaker opens to create a power mismatch by adding reactive power [25]. It is unlikely that capacitors could be used as solution for fast acting energy storage as these could react with the filter impedance of the inverter and cause unwanted resonance.

2. Problem Definition

Despite the published work aimed at improving anti-islanding protection, the UK Energy Storage system is still heavily tied to traditional RoCoF techniques. Fast acting energy storage connected to the grid system has to use ROCOF or vector shift protection as part of the grid connection requirements. The settings associated with these are not designed for fast acting storage and therefore plant connected in this

way will trip unpredictably on a frequent basis; called nuisance tripping.

An additional complication is that although the RoCoF protection should not trip when the battery is importing, existing protection devices have no discrimination between import and export.

This paper is novel because it tries to quantify those impacts based on real world operation of a 2MW energy storage system and suggests RoCoF settings that could be applied without major changes to the methodology behind RoCoF anti-islanding protection as a mechanism for reducing nuisance trips.

This paper is organised as follows. Section 3 investigates why spurious tripping is an issue for fast acting energy storage. Section 4 introduces the Willenhall Energy Storage System (WESS) – a 2MW lithium-titanate battery system – that has been used to generate the practical results in this paper. Section 4 introduces a single-phase equivalent-circuit model of the WESS using simulink. Section 5 compares the model results with those obtained from fast power switching of the WESS between import and export to validate the model. This model is then used in Section 6 to investigate the likelihood of nuisance tripping for the proposed protection settings to determine the likelihood of nuisance tripping on the Network.

3. Reason for Nuisance Trips

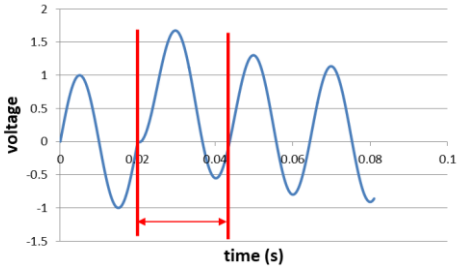

Fig. 1. Simplified waveform at the point of measurement for connection of the BESS to the Grid

Fig. 1 is the standard waveform for a fault occurring at zero switching but this is also representative of the waveform that would be attained for a sudden change in import/export power. This paper considers power swings and different values of power angle at which this power swing occurs due to the presence of additional capacitance in the inverter. Fig. 2 shows a simplified model of the WESS connected to the network with the impedances of the key elements lumped together. The battery energy storage system (BESS) is connected to an inverter, which exports power through a filter to a transformer to the grid.

The equations of the circuit are as follows:

$$V_b - V_c = L_1 \frac{\delta I_1}{\delta t} \tag{1}$$

$$I_1 - I_2 = C_1 \frac{\delta V_c}{\delta t} \tag{2}$$

$$V_c - V_G = L_2 \frac{\delta I_2}{\delta t} + L_3 \frac{\delta I_2}{\delta t} + I_2 R_1 + I_2 R_2 + L_4 \frac{\delta I_2}{\delta t} \tag{3}$$

$$\frac{\delta I_2}{\delta t} = \frac{V_c}{(L_2+L_3+L_4)} - \frac{V_G}{(L_2+L_3+L_4)} - \frac{I_2(R_1+R_2)}{(L_2+L_3+L_4)} \tag{4}$$

In addition, the measured voltage at the protection relay can be found from,

$$V_m - V_G = I_2 R_2 + L_4 \frac{\delta I_2}{\delta t} \tag{5}$$

The following set of equations needs to be solved in order to calculate this measured voltage.

$$\begin{vmatrix} \delta V_c/\delta t \\ \delta I_1/\delta t \\ \delta I_2/\delta t \end{vmatrix} = \begin{vmatrix} 0 & \frac{1}{C_1} & -\frac{1}{C_1} \\ -\frac{1}{L_1} & 0 & 0 \\ \frac{1}{L_2+L_3+L_4} & 0 & -\frac{R_1+R_2}{L_2+L_3+L_4} \end{vmatrix} \begin{vmatrix} V_c \\ I_1 \\ I_2 \end{vmatrix} + \begin{vmatrix} 0 \\ V_b/L_1 \\ \frac{-V_G}{(L_2+L_3+L_4)} \end{vmatrix} \tag{6}$$

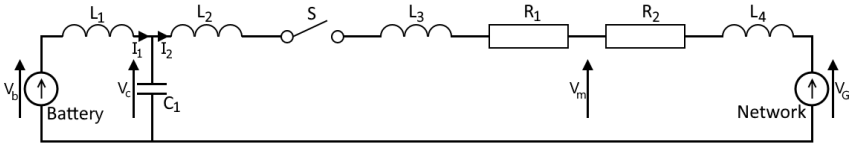

R1 and L3 = LV impedance of circuits S = Power Import/Export Changeover Switch L1, L2 and C1 = ESS filter impedance
R2 and L4 = Transformer and Grid Network impedance referred to LV side of transformer
Vb = Battery Inverter Voltage Vc = Capacitor Voltage Vm = Measurement Voltage (Relay) location VG = Grid Voltage
I1 = ESS Current I2 = Grid Current

Fig. 2. Simplified network model

The resultant waveform produced during connection to the grid is a transient state of similar form to that produced under fault, in that it has both DC and AC components due to the presence of the inductance and the subsequent L/R time constant, as shown in Fig. 1 in exaggerated form.

It is the presence of the DC component, which affects where the zero crossing is detected. The longer time to detecting the zero crossing shown by the arrow appears to the protection as a change in phase shift or frequency. The detection of and subsequent analysis of the zero crossing and its use in the LoM protection is the reason behind the nuisance trip. The value of the DC component is dependent on when the switching occurs in relation to the phase angle of the sine wave component of the grid voltage.

Once the zero crossing has been detected, this value is used to determine the vector shift or RoCoF configuration values. Obviously, Fig. 1 is a simplification of the waveform that would be produced, as there is also capacitance present in the system resulting in a more complex waveform. The research question then becomes two fold; what would the settings need to be to ensure no nuisance tripping and how would this vary across different BESS schemes?

4. Experimental Platform

The WESS is a collaborative research facility, funded by the UK EPSRC under the 'Capital for great technologies call'. The full-scale system, owned and operated by the University of Sheffield, includes a 2MW, 1MWh Toshiba lithium-titanate battery system [26], which is interfaced to a 2MVA ABB inverter, connected to the grid through an 11kV feed at the Willenhall primary substation, via a step-up isolation transformer as shown in Fig. 4. Fig. 3 shows the site including the 2MW battery container, isolation transformer and inverter container.

The system was designed to be a fast acting energy storage system and is able to transition from full import to full export and vice versa in a sub-cycle time scale. At peak power output, the system can provide a 4MW power swing within 2 cycles. The WESS operates UK under national power demand and frequency response schemes up to its rated capacity.

Fig. 3. Willenhall energy storage system

The WESS G59 protection system includes the distribution network operator (DNO) witness tested Woodward MFR1 relay, which is used for the day-to-day running of the system. As part of this testing, an

additional Deep Sea Electronics (DSE) P100 protection relay was installed in parallel with the Woodward relay, as shown in Fig. 5. This relay provides greater setup flexibility and access to data.

The 1MWh battery system was operated for a number of cases to mimic real-world operational modes,

- 0 – 2MW Export
- 0 – 2MW Import
- 2MW Import – 2MW Export
- 2MW Export – 2MW Import

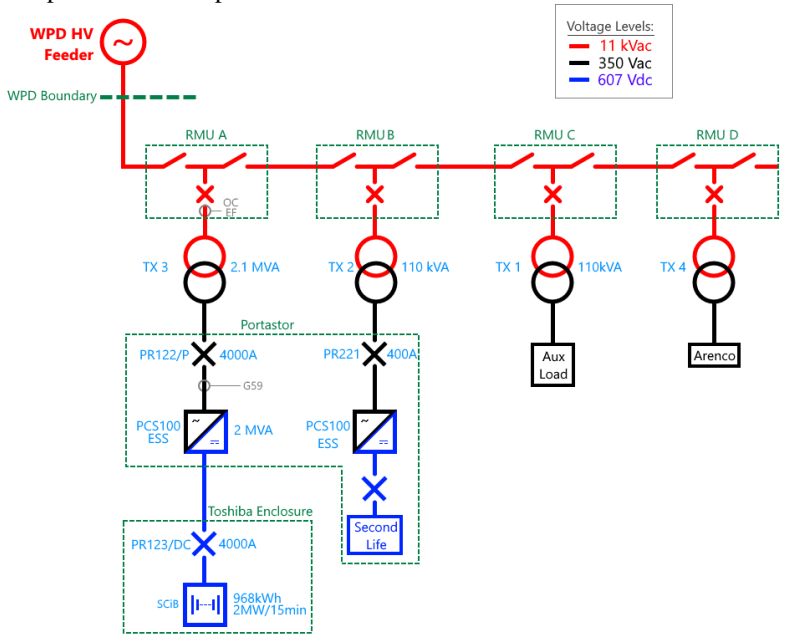

Fig. 4. WESS single line diagram

The data from which was used to validate the created Simulink model. To capture the data, a LeCroy oscilloscope was connected using three differential voltage probes to the three line voltages and used to capture the waveforms of the measurement data during system operation. A fourth probe was used to generate the trigger point for a trip signal from the DSE relay. The DSE relay was setup to trip on RoCoF excursions and to record both the peak vector shift and RoCoF seen by the relay.

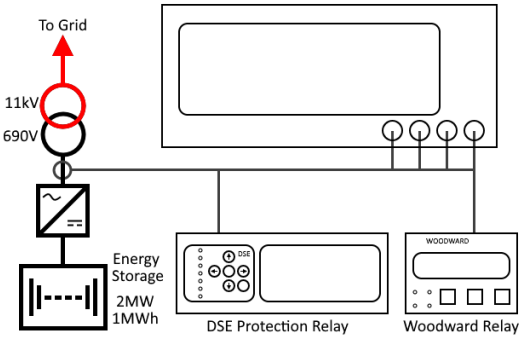

Fig. 5. G59 protection system

5. Simulink Model of Willenhall

A single-phase equivalent model of the WESS was produced in Matlab Simulink 2017a, as shown in

Fig. 6. The impedance values of the system were estimated from a combination of manufacturer's data and calculations of cable impedance. These are detailed in Table 1, they represent an approximation of the parameters of the system. The filter impedance is not explicitly known but has been estimated. The model was run using a fixed time step and the inverter voltage was subject to a step change to simulate a change in power to match that obtained experimentally. The grid voltage was assumed constant throughout the modelling and represented as a voltage source with a series impedance. The value of this impedance is adjusted to represent a strong grid and a weak grid. The voltage at the measurement location was noted and compared to that obtained experimentally under the following tests.

Table 1. Simulink Model Parameters

	Prefix	Value
LV Resistance	R1	1.44mΩ
ESS Filter Capacitance	C1	180μF
ESS Filter Inductance	L1	94.0 μH
ESS Filter Inductance	L2	47.0 μH
LV Inductance	L3	59.0 μH
Values referred to the LV side	Prefix	Value
Tx & Grid Resistance	R2	2.25m
Strong Grid Tx & Grid Inductance	L4	1.60 μH
Weak Grid Tx & Grid Inductance	L4	8.00 μH

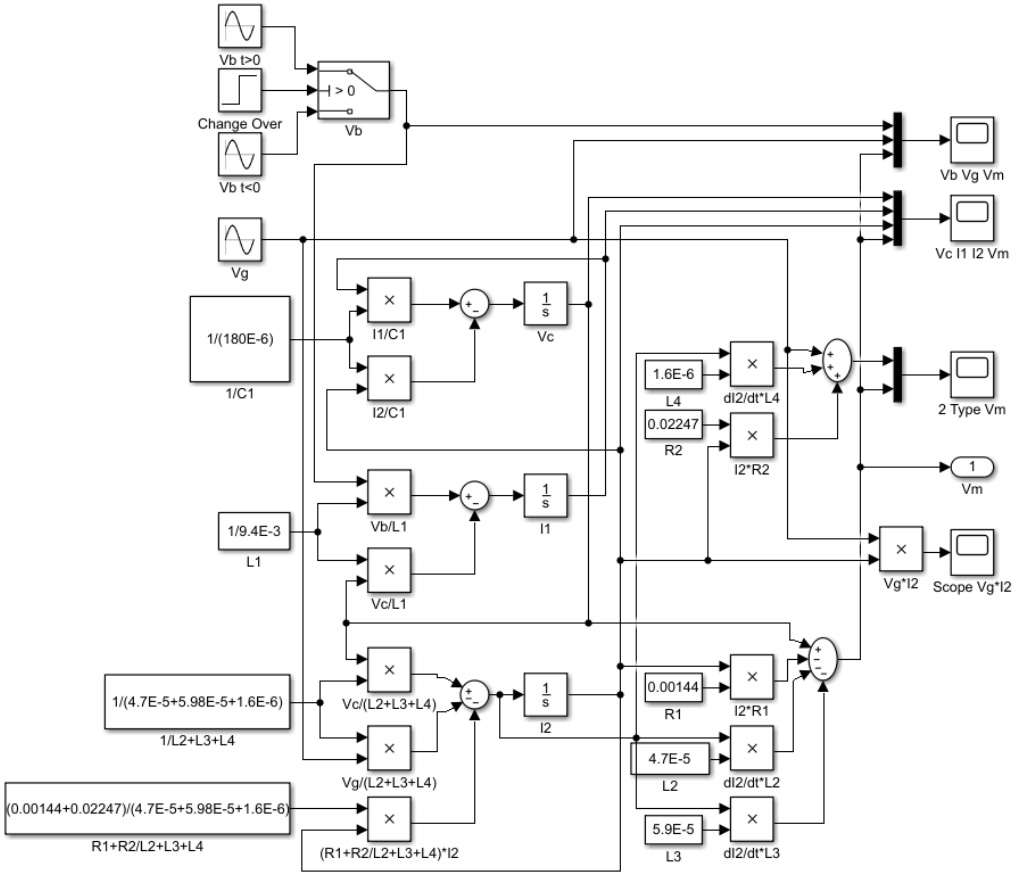

Fig. 6. Simulink model of the WESS

6. Experimental Validation

Experimental tests were carried out according to the testing schedule shown in Table 2, to enable validation of the theoretical model against four real world operational cases. Each test needed to be run a couple of times, as the DSE relay did not always detect a trip condition, even when the Woodward relay tripped. This highlights a discrepancy in the sensitivities of the relays, which is assumed a function of the different filtering and analytical techniques employed by each manufacturer to calculate the LoM parameters.

Table 2. Experimental Testing Schedule

		DSE RoCoF Settings		DSE Relay		Woodward Relay
#	Power	Hz/s	Filter Cycles	Vector Shift	RoCoF	RoCoF
1	0 – 2 MW Export	0.125	20	5.4°	0.39 Hz/s	Trip
2	2MW Import – 2MW Export	0.125	13	7.6°	1.21 Hz/s	Trip
3	0 – 2 MW Import	0.125	13	5.4°	0.53 Hz/s	Trip
4	2MW Export – 2MW Import	0.125	13	5.8°	0.99 Hz/s	Trip

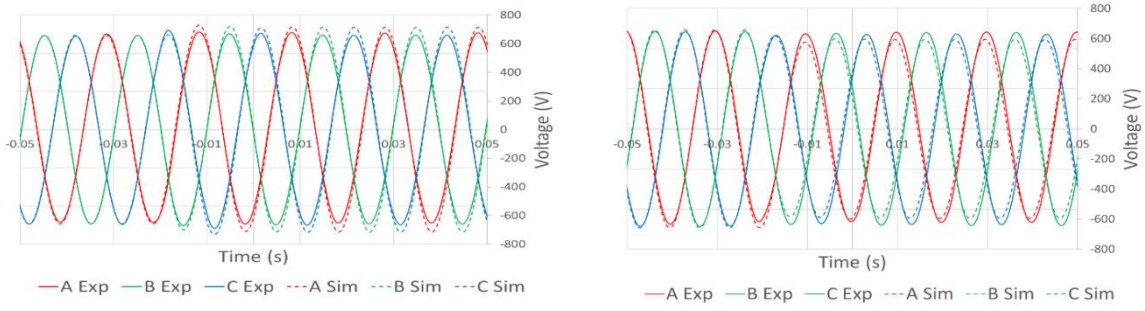

(a) (b)

Fig. 7. Experimental and simulated results: (a) 0 – 2MW Export; (b) 0 – 2MW Import

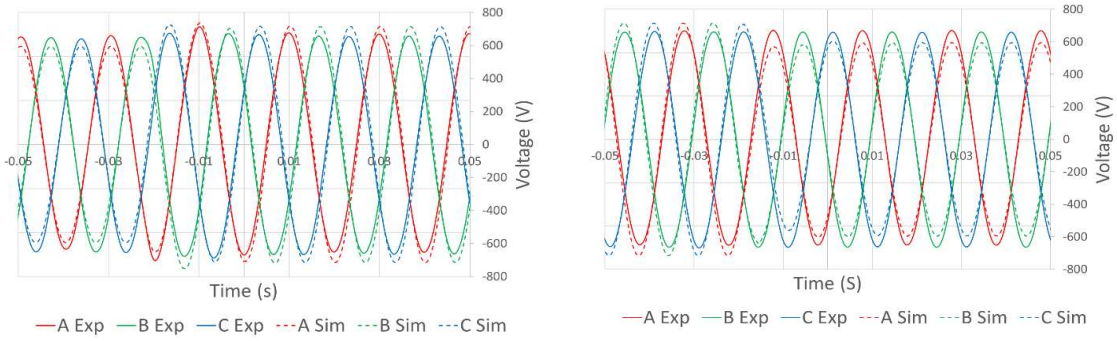

(a) (b)

Fig. 8. Experimental and simulated results: (a) 2MW Import – 2MW Export; (b) 2MW Export – 2MW Import

Where the DSE relay did detect a trip, the corresponding peak vector shift and RoCoF values measured by the relay were recorded in Table 2 along with whether the Woodward relay tripped.

Fig. 7 and Fig. 8 show the graphs of the modelled voltage at the point of measurement against the scope traces. The trip signal is registered by the scope at time t=0s and therefore, the event that leads to the trip is approximately 60ms prior to this due to fault detection, calculation and relay operation. In all cases, the simulated waveform follows the same trend as the experimental waveform and the change in voltage and the DC-offset components leading to incorrect tripping can be seen. “A Exp”, “B Exp” and “C Exp” are the three experimental line voltages while “A Sim”, “B Sim” and “C Sim” are the three simulated line voltages.

It is assumed that the grid voltage and battery inverter voltage magnitude are constant. However, in reality these change with time and are partly the reason why the voltages in Fig. 8 (b) are less accurate. As the voltage is kept constant the “generator angle”, δ, - the angle between the inverter and the grid - was adjusted in order to simulate the change in power condition of the BESS. As the inverter control system within the ABB inverter is proprietary code, it is not known how accurate a representation this is of changing the power setting. However, power in the model was crosschecked to ensure it was a suitably representative value of the test.

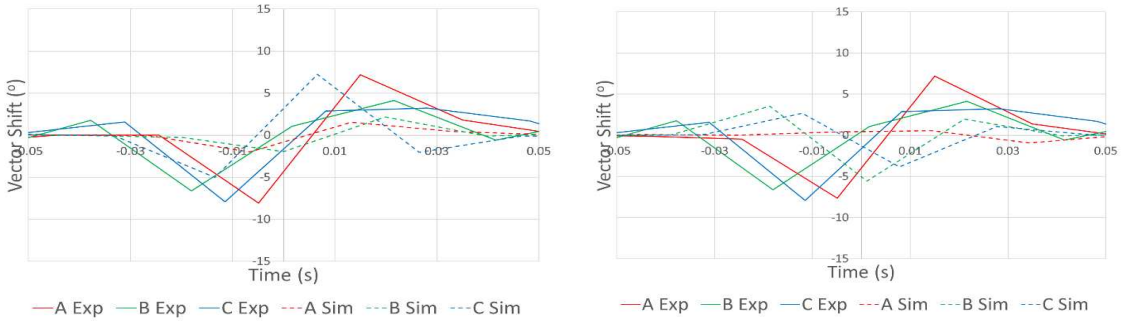

(a) (b)

Fig. 9. Calculated experimental and simulated vector shift: (a) 0 – 2MW Export; (b) 0 – 2MW Import

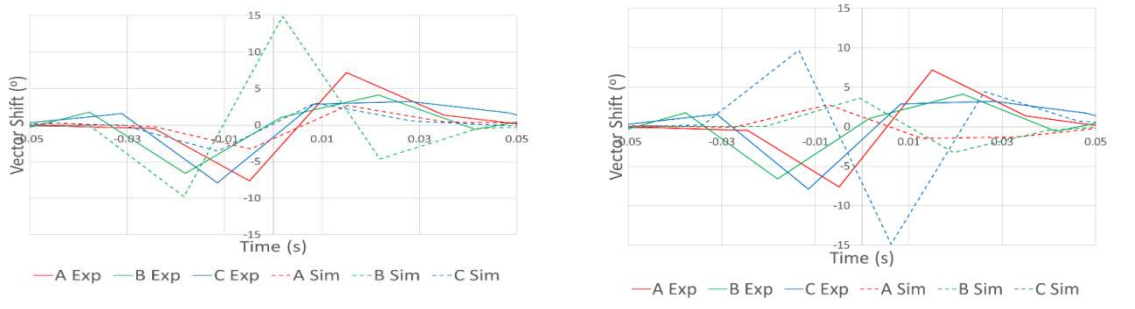

(a) (b)

Fig. 10. Calculated experimental and simulated vector shift: (a) 2MW Import – 2MW Export; (b) 2MW Export – 2MW Import

These figures show a standard three phase waveform with 120o phase shift as expected. The resultant impact on the waveform following a shift in Power setting – either import or export – is visible at the 0s

time setting.

The calculated values of vector shift under the experimental test and simulated calculations are shown in Fig. 9 and Fig. 10. The order of magnitude of the vector shift value is similar between the experimental and simulated values; however, the timing is displaced. It is thought that this is related to the difficulty of directly determining when the inverter power setting has changed.

The DSE relay recorded a value of voltage shift between 5° and 8°. The experimental and model values over the same tests (with no filtering) yielded values closer to 7° to 10°. These values are greater than the 6° of the standard for connection to a strong grid but lower than the 12° values, which would be allowed for a weak grid connection. Unfortunately, as the WESS is at a primary substation close to a bulk supply point, it definitely counts as a strong grid situation.

It is difficult to determine what the corresponding RoCoF value would be, especially in view of the different filtering settings. A reasonable guess based on the data is shown in Table 3.

Table 3. Simulated vs experimental RoCoF test results

#	Power	Simulated	Experimental
1	0 – 2 MW Export	2.7 Hz/s	4.4 Hz/s
2	2MW Import – 2MW Export	5.4 Hz/s	4.3 Hz/s
3	0 – 2 MW Import	3.0 Hz/s	4.3 Hz/s
4	2MW Export – 2MW Import	7.8 Hz/s	4.3 Hz/s

These values are much higher than those reported by the DSE relay (0.4 – 1.3Hz/s) as the model results are showing values of up to 8Hz/s. These values are based on matching the phase of the switching of inverter set point in the model as close as possible to the switching of the experimental data; though, in reality this phase is not controlled.

Due to the presence of estimated data, it is believed that the results of the model are sufficiently accurate to allow further studies to be undertaken. Values out by more than 10° would be cause for concern.

7. Switching Angle Perturbance Simulation

The impact of the switching angle on the measured vector shift and RoCoF was investigated including different filtering cycles (0, 13 & 20) for the RoCoF. Fig. 11 shows the impact of switching at different angles on the modelled value of maximum vector shift and RoCoF, respectively. The test was carried out for a 0-2MW export case with the B phase results shown. Other parameters that affect the vector shift and RoCoF values include the strength of the grid. These values were generated for a strong grid. However, similar values for a weak grid are shown in Fig. 12.

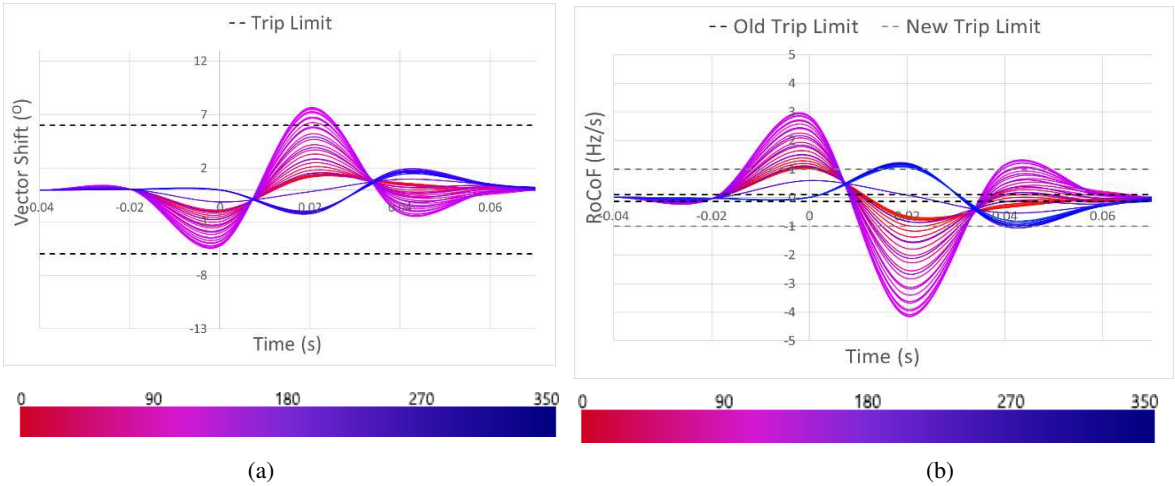

Fig. 11. Simulated impact of switching angle: (a) Vector shift; (b) RoCoF

Table 4. Strong grid switching angle results

	Best	Worst	Trip
Vector Shift	0.97°	7.64°	22%
RoCoF (0)	6.83 Hz/s	53.8 Hz/s	100%
RoCoF (13)	0.53 Hz/s	4.14 Hz/s	97%
RoCoF (20)	0.34 Hz/s	2.69 Hz/s	50%

It is clear from the results that the worst case occurs at 80° for phase A, 200° for phase B and 320° for phase C. Table 4 shows the best and worst results along with the percentage of angles that result in a trip. Therefore, to avoid all forms of nuisance tripping at the WESS, the RoCoF setting would need to be at least 4.2Hz/s and the vector shift setting would need to be 7.7°. Table 5 shows the overall trip percentage over the three phases, keeping the settings at their current limits would result in a trip on one of the phases 33% of the time by vector shift and 100% of the time through RoCoF.

Table 5. Strong grid three phase trip percentage

	Vector Shift	RoCoF (0)	RoCoF (13)	RoCoF (20)
Trip	67%	100%	100%	100%

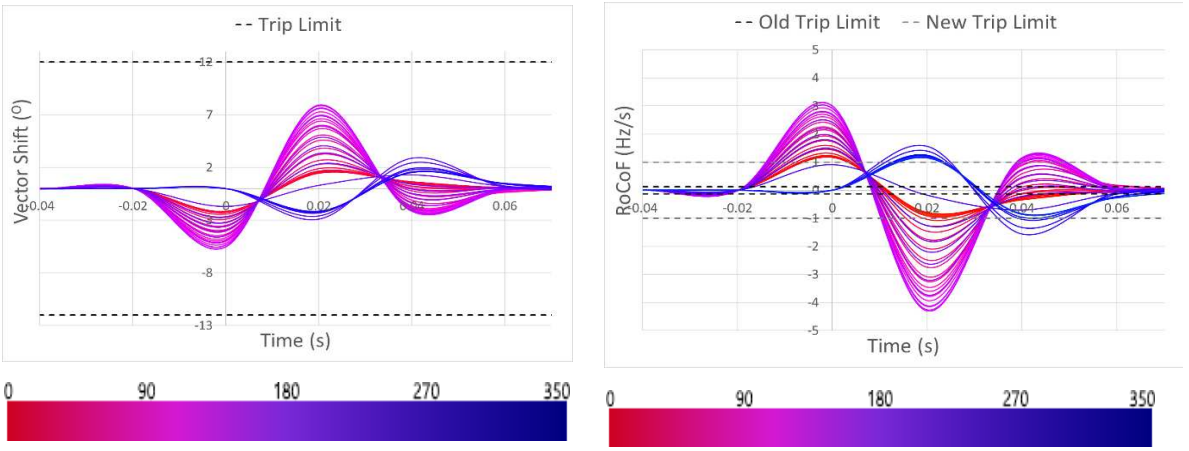

(a) (b)

Fig. 12. Simulated impact of switching angle in a weak grid: (a) Vector shift; (b) RoCoF

Table 6. Weak Grid Switching Angle Results

	Best	Worst	Trip
Vector Shift	1.27°	7.91°	0%
RoCoF (0)	8.87 Hz/s	55.8 Hz/s	100%
RoCoF (13)	0.68 Hz/s	4.29 Hz/s	97%
RoCoF (20)	0.44 Hz/s	2.79 Hz/s	57%

This is clearly undesirable and if the BESS were operating under a fast response balancing mechanism service would result in penalty charges to the operator of the equipment. This would affect the business case for the BESS and would need to be considered in the financial calculations. The graphs indicate that the introduction of a 500ms time delay on RoCoF settings will prevent the nuisance trips as the graphs show that the system stabilises within about 5 cycles (or 100ms).

For a weak grid, the results are slightly different. Table 6 details the results and the worst-case scenario occurs at a different point of 90° for phase A, 210° for phase B and 330° for phase C, and the RoCoF setting would need to be at least 4.4Hz/s and the vector shift setting would need to be 8° to avoid nuisance tripping. Table 7 shows the overall trip percentage over the three phase's for a weak grid, keeping the settings at the current limits would result in a trip on one of the phases 0% of the time by vector shift and 100% of the time through RoCoF.

Table 7. Weak grid three phase trip percentage

	Vector Shift	RoCoF (0)	RoCoF (13)	RoCoF (20)
Trip	0%	100%	100%	100%

Tables 4 – 7 backed by the simulation in fig. 11 and fig. 12 show that the likelihood of the system tripping on current vector shift and RoCoF settings is unacceptably high. This would cause problems for a grid system operator relying on the response of energy storage to assist with frequency control.

8. Conclusion

In theory, the battery system should not trip on LoM protection when it is importing, as this is not a requirement. However, the relay has no mechanism for differentiating between importing and exporting resulting in an increase in nuisance trips over and above what would occur under current statutory limits.

As all relays have proprietary code, they do not all react in the same way during LoM detection. At the WESS, the Woodward relay tripped out far more frequently than the DSE relay and therefore in the course of this work there were far more nuisance trips than recorded trips.

It is difficult to match the simulated and experimental results, as the control system implementation in the inverter is not explicitly published. Similarly, the mechanism for calculating the LoM protection is proprietary and so difficult to replicate. The uncertainty in the filtering and control behind the implementation gives differences between reported relay settings and that determined from experimental waveforms. No official standard exists to ensure consistency across relay manufacturers.

However, what is clear is that fast acting power swings of energy storage results in nuisance trips, which are unrelated to changes in frequency caused by zero crossing detection of waveforms with a DC component. Simulated results indicate that settings would need to be adjusted to at least 4.2Hz/s RoCoF and 7.7° vector shift in order to avoid tripping in a strong grid, and 4.4 Hz/s RoCoF and 8° vector shift in a weak grid. Keeping the settings where they are would result in nuisance tripping approximately 100% of the time under a fast acting operation. The WESS inverter controller has a programmable power ramp rate to avoid nuisance trips. However, if energy storage is to be fully utilised for grid stability, then it is important to ensure that it can operate to its full fast acting capability without constraint.

Conflict of Interest

The authors declare no conflict of interest.

Author Contributions

Simon Royston designed and wired the experimental setup, Simon Royston, Dani Strickland and Shahab Nejad undertook the experimental data collection, Simon Royston and Dani Strickland undertook the modelling, analysis and documenting of the work, David A Stone, Daniel Gladwin and Martin Foster reviewed the work and dealt with the operational and safety aspects of the site. All authors had approved the final version.

Acknowledgements

This work was supported by the UK Engineering and Physical Sciences Research Council (EPSRC) grant EP/N032888/1. Special thanks to Western Power Distribution and Deep Sea Electronics for their support and providing a DSEP100 mains protection relay.

References

[1] Energy Network Association, "Engineering Recommendation G83," 2012.

[2] Energy Networks Association, "Engineering Recommendation G59/3-2," 2015.

[3] Motter D and Vieira JCM. The setting map methodology for adjusting the DG anti-islanding protection considering multiple event. *IEEE Transactions on Power Delivery,* 2018;33(6): 2755-2764.

[4] Roscoe AJ, Dysko A, Marshall B, Lee M, Kirkham H, and Rietveld G. The case for redefinition of frequency and ROCOF to account for AC power system phase steps. in *IEEE International Workshop on Applied Measurements for Power Systems (AMPS)*, Liverpool, 2017.

[5] Nassif A. and Madsen C. A real case application of ROCOF and vector surge relays for anti-islanding protection of distributed energy resources. in *IEEE Electrical Power and Energy Conference (EPEC)*, Saskatoon, 2017.

[6] National Grid, *Working Group GC0035/GC0079.*

[7] Ofgem, "DC0079 - Frequency changes during large disturbances and their impact on the total system," Office of Gas and Electricity Markets, London, 2017.

[8] Hatata A, Abd-Raboh EH and Sedhom B. A review of anti-islanding protection methods for renewable distributed generation systems. *Journal of Electrical Engineering,* vol. 16, no. 1, 2016.

[9] Bright CG, "COROCOF: Comparison of rate of change of frequency protection. a solution to the detection of loss of mains," in *7th International Conference on Developments in Power Systems Protection (DPSP)*, Amsterdam, Netherlands, 2001.

[10] Salman SK, King DJ and Weller G. New loss of mains detection algorithm for embedded generation using rate of change of voltage and changes in power factors. in *7th International Conference on Developments in Power Systems Protection(DPSP)*, Amsterdam, Netherlands, 2001.

[11] Marchesan G, Muraro MR, Cardoso G, Mariotto L and De Morais AP. Passive method for distributed-generation island detection based on oscillation frequency. *IEEE Transactions on Power Delivery,* 2016; 31(1): 138-146.

[12] Gupta P, Bhatia RS and Jain DK. Active ROCOF relay for islanding detection. *IEEE Transactions on Power Delivery,* 2017; 32(1): 420-429.

[13] Liu H, Wang B, Zhao J. Wang KL and Li Y. A setting method of frequency bias coefficient for interconnected power grid based on shapley value, in *IEEE PES Asia-Pacific Power and Energy Conference*. Xi'an, 2016.

[14] Wen B, Boroyevich D, Burgos R, Shen Z and Mattavelli P. Impedance-based analysis of active frequency drift islanding detection for grid-tied inverter system. *IEEE Transactions on Industry Applications,* 2016; 52(1): 332-341.

[15] Bower W. and Ropp M. Evaluation of islanding detection methods for photovoltaic utility-interactive power systems.IEA-PVPS T5-09: 2002, 2002.

[16] Safari A. A novel islanding detection technique for distributed generation. *International Journal of Advanced Science and Technology,* 2013;51: 1-10.

[17] Cintuglu MH and Mohammed OA. Islanding detection in microgrids. in *2013 IEEE Power & Energy Society General Meeting*, 2013.

[18] O'Kane P and Fox B. Loss of mains detection for embedded generation by system impedance monitoring. in *6th International Conference on Developments in Power Systems Protection*, Nottingham, UK, 1997.

[19] Cooper CB. Standby generation problems and prospective gains from parallel running. in *Power System Protection*, Singapore, 1989.

[20] Li C, Savulak J and Reinmuller R. Unintentional islanding of distributed generation-operating experiences from naturally occurred events. *IEEE Transactions on Power Delivery,* 2014; 29(1): 269-274.

[21] Trindade FCL, Do Nascimento KV and Vieira JCM. Investigation on voltage sags caused by dg anti-islanding protection. *IEEE Transactions on Power Delivery,* 2013; 28(2): 972-980.

[22] Roscoe AJ, Blair SM, Dickerson B and Rietveld G. Dealing with front-end white noise on differentiated measurements such as frequency and ROCOF in power systems. *IEEE Transactions on Instrumentation and Measurement,* 2018; 67(11): 2579-2591.

[23] Castello P, Ferrero R, Pegoraro PA. and Toscani S. Effect of unbalance on positive-sequence synchrophasor, frequency, and ROCOF estimations. *IEEE Transactions on Instrumentation and Measurement,* 2018;67(5): 1036-1046.

[24] Khanbabapour S, and Hamedani GME. Synchronous DG planning for simultaneous improvement of technical, overcurrent, and timely anti-islanding protection indices of the network to preserve protection coordination. *IEEE Transactions on Power Delivery,* 2017; 32(1): 474-483.

[25] Bejmert D and Sidhu TS. Investigation into islanding detection with capacitor insertion-based method. *IEEE Transactions on Power Delivery,* 2014; 29(6); 2485-2492.

[26] Rogers D, Gladwin DT, Stone D, Strickland D and Foster M. Willenhall energy storage system: Europe's largest research-led lithium titanate battery, IET Engineering and Technology Reference, 2017.